A new method of calculating the orbital angular momentum spectra of Laguerre–Gaussian beams in channels with atmospheric turbulence*

Xiao-zhou Cui(崔小舟)[1,2], Xiao-li Yin(尹霄丽)[1,2,3,†], Huan Chang(常欢)[1,2], Zhi-chao Zhang(张志超)[1,2], Yong-jun Wang(王拥军)[1,2,3], and Guo-hua Wu(吴国华)[1,3]

[1] *School of Electronic Engineering, Beijing University of Posts and Telecommunications, Beijing* 100876, *China*
[2] *Beijing Key Laboratory of Space-Ground Interconnection and Convergence, Beijing University of Posts and Telecommunications, Beijing* 100876, *China*
[3] *State Key Laboratory of Information Photonics and Optical Communications, Beijing University of Posts and Telecommunications, Beijing* 100876, *China*

(Received 18 May 2017; revised manuscript received 18 July 2017; published online 30 September 2017)

Studying orbital angular momentum (OAM) spectra is important for analyzing crosstalk in free-space optical (FSO) communication systems. This work offers a new method of simplifying the expressions for the OAM spectra of Laguerre–Gaussian (LG) beams under both weak/medium and strong atmospheric turbulences. We propose fixing the radius to the extreme point of the intensity distribution, review the expression for the OAM spectrum under weak/medium turbulence, derive the OAM spectrum expression for an LG beam under strong turbulence, and simplify both of them to concise forms. Then, we investigate the accuracy of the simplified expressions through simulations. We find that the simplified expressions permit accurate calculation of the OAM spectrum for large transmitted OAM numbers under any type of turbulence. Finally, we use the simplified expressions to analytically address the broadening of the OAM spectrum caused by atmospheric turbulence. This work should contribute to the concise theoretical derivation of analytical expressions for OAM channel matrices for FSO-OAM communications and the analytical study of the laws governing OAM spectra.

Keywords: orbital angular momentum (OAM) spectrum, atmospheric turbulence, free-space optical (FSO) communications

PACS: 42.68.Bz, 42.68.Ay, 42.25.Dd **DOI:** 10.1088/1674-1056/26/11/114207

1. Introduction

Over the last 20 years, free-space optical (FSO) communication systems have been developed in an attempt to satisfy the enormous demand for data capacity, and thus, interest in orbital angular momentum (OAM) characteristics is growing.[1,2] Beams with different OAM number l, which is an arbitrary integer, are orthogonal to each other, which leads to the possibility of enlarging the channel capacity in OAM-multiplexed communications.

A practical implementation of a simple FSO-OAM system was reported in 2004.[3] Wang experimentally demonstrated the potential of OAM multiplexing for high-speed communications.[4] Several outdoor demonstrations have also been reported,[5,6] and an FSO-OAM system with a communication distance of 143 km has been realized.[7] All of these works confirm the feasibility of FSO using OAM multiplexing. However, implementations of this strategy face many difficulties, such as atmospheric turbulence, beam divergence, and offset between the transmitters and receivers,[8–13] which can induce the broadening of the OAM spectrum and degrade the performance of the FSO–OAM communication systems. Several previous works addressing beams traveling through atmospheric turbulence have proposed a group of models for describing atmospheric characteristics.[14–23] The OAM spectrum measures the proportion of power remaining in a transmitted channel and crosstalk with adjacent channels in an FSO-OAM communication system, and the OAM spectrum can be used to formulate a channel matrix, which is important for calculating the channel capacity. Thus, studying the theoretical broadening of OAM spectra is necessary.[12] One common method used to calculate the OAM spectrum is based on conjugate spiral phase plates and the principle of orthogonality.[12] In other theoretical studies, probability-based expressions for the OAM spectrum have been derived.[1,10,17–19] In most such studies, based on Laguerre–Gaussian (LG) beams and other types, such as Bessel–Gauss beams, statistical models have been used to analyze and derive precise but complex results for atmospheric channels via model decomposition.[1,10,20–23] The results involve the infinite integration of Bessel functions, which ensures their accuracy; however, the calculation required is enormous, and further derivation is difficult.

In this work, we mainly focus on the broadening of the OAM spectrum caused by atmospheric turbulence. First, we propose a method called the fixed-radius method (FRM) to simplify the expression for the OAM spectrum of an LG beam in a channel with weak/medium atmospheric turbulence. We also derive the expression for the OAM spectrum of an LG

*Project supported by the National Natural Science Foundation of China (Grant Nos. 61575027 and 61471051).
†Corresponding author. E-mail: yinxl@bupt.edu.cn
© 2017 Chinese Physical Society and IOP Publishing Ltd

beam in a channel with strong atmospheric turbulence and use the FRM to simplify the expression. Then, we define the overall error e to compare the calculation results of the FRM and the elementary formula method (EFM).[1] Finally, we use the simplified expressions to analytically explain the broadening of the OAM spectrum.

This work is expected to contribute to studies of FSO-OAM communications, such as concise theoretical derivations of the OAM channel matrix. Additionally, the resulting expressions can be used to analyze the laws governing the OAM spectrum under atmospheric turbulence.

2. FRM for OAM spectrum calculation

The most common types of vortex beams that are used to carry OAM are LG beams because LG beams are easily realized. Because of the in-axis symmetry of the distribution, an LG beam is described using cylindrical coordinates, and the field distribution for a radial mode of $p=0$ can be expressed as[13]

$$u_{l_0,\mathrm{free}}(r,\phi,z)=R_{l_0}(r,z)\exp(\mathrm{i}l_0\phi), \tag{1}$$

where

$$R_{l_0}(r,z)=\sqrt{\frac{2}{\pi|l_0|!}}\frac{1}{\omega(z)}\exp\left[-\left(\frac{r^2}{\omega^2(z)}\right)\right]\left[\frac{\sqrt{2}r}{\omega(z)}\right]^{|l_0|}\times\exp\left\{\mathrm{i}(|l_0|+1)\tan^{-1}\left(\frac{z}{z_\mathrm{R}}\right)-\mathrm{i}\left[\frac{r^2}{\omega^2(z)}\right]\frac{z}{z_\mathrm{R}}\right\},$$

and l_0 is the angular mode number. The $1/\mathrm{e}$ radius of the Gaussian term is given by $\omega(z)=\omega_0\sqrt{1+z^2/z_\mathrm{R}^2}$, where ω_0 is the beam waist, $z_\mathrm{R}=\pi\omega_0^2/\lambda$ is the Rayleigh range, λ is the wavelength, and $(|l_0|+1)\tan^{-1}(z/z_\mathrm{R})$ is the Gouy phase.

Figure 1(a) shows the intensity profile of an OAM beam with p=0. Figure 1(b) shows the corresponding intensity distribution; the shape of the beam is a doughnut-like ring, and most of the energy is focused within the ring. Figure 1(c) presents the intensity distribution after it has been disturbed by atmospheric turbulence. The beam remains doughnut-like in shape despite the perturbation. Figure 1(a) indicates extreme points in the intensity profile. LG modes with a radial index of zero are single-ringed annular modes. The intensity profile of the ring resembles a narrow window because most of the power is concentrated in a narrow annulus. By solving the equation $\partial|u_l(r,\phi,z)|^2/\partial r=0$, we can obtain the radius of the ring at which the intensity is a maximum[13]

$$r'=\sqrt{\frac{|l_0|}{2}}\omega(z). \tag{2}$$

If we fix the radius to r', the doughnut-like shape becomes a thin ring, and the dimensionality (r,ϕ,z) decreases to (ϕ,z). The communication distance z can often be regarded as a constant; in this case, the dimensionality becomes only (ϕ), and we can easily derive the corresponding equations. Although the simplified equations ignore some of the energy in the beam, most of the energy is concentrated at the radius r'. We will demonstrate the validity of this approach in the following sections.

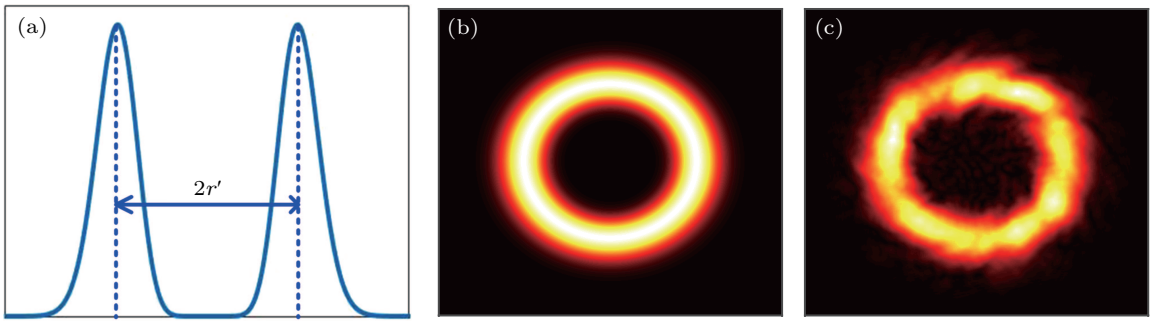


Fig. 1. (color online) Characteristics of OAM beams: (a) intensity profile of a pure OAM beam, (b) intensity distribution of a pure OAM beam, and (c) intensity distribution of an OAM beam under atmospheric turbulence.

3. Analysis of the OAM spectrum under atmospheric turbulence using the FRM

In this section, we first review the expression for the OAM spectrum under weak/medium turbulence and simplify it. Then, we derive the expression for the OAM spectrum of an LG beam under strong turbulence and simplify it as well.

3.1. Expression for the OAM spectrum under weak/medium turbulence derived using the FRM

For regions with weak/medium atmospheric turbulence, we can use the Rytov approximation to obtain the complex amplitude of a beam disturbed by the weak/medium turbulence as follows:[1]

$$u_{l,\mathrm{wm}}(r,\phi,z)=u_{l_0,\mathrm{free}}(r,\phi,z)\exp[\psi(r,\phi,z)], \tag{3}$$

where $\psi(r,\phi,z)$ is the complex-phase turbulence perturbation and l_0 is the transmitted OAM number. The OAM spectrum will broaden because of $\psi(r,\phi,z)$. The OAM probability density, which we call the EFM result, is given by[1]

$$C(l) = \frac{2\pi A^2}{\omega^2(z)}\int_0^R \left[\frac{\sqrt{2}r}{\omega(z)}\right]^{2|l_0|} \times \exp\left[\frac{-2r^2}{\omega(z)^2}-\frac{2r^2}{r_0^2}\right]\times \mathrm{I}_{l-l_0}\left(\frac{2r^2}{r_0^2}\right) r\,\mathrm{d}r, \quad (4)$$

where $A=\sqrt{2/\pi(|l_0|)!}$, R is the radius of the receiver aperture, I_n is the modified Bessel function of the first kind of integer n, and

$$r_0 = \left[1.46k^2\int_0^z C_n^2(z')\left(1-\frac{z'}{z}\right)^{5/3}\mathrm{d}z'\right]^{-3/5} \quad (5)$$

is the coherence radius of the spherical wave. Here, z is the transmission distance, and $C_n^2(z')$ is the refractive index structure parameter, for which one of the most widely used models is the Hufnagel–Valley model[24]

$$\begin{aligned} &C_n^2(z'\cos\alpha)\\ &= 8.148\times10^{-56}v^2(z'\cos\alpha)^{10}\exp(-z'\cos\alpha/1000)\\ &\quad +2.7\times10^{-16}\exp(-z'\cos\alpha/1500)\\ &\quad +C_n^2(0)\exp(-z'\cos\alpha/100), \end{aligned} \quad (6)$$

where $C_n^2(0)$ is the refractive index structure parameter that is characteristic of the ground, α is the zenith angle, and v is the square root of the wind speed. Over short time intervals at a fixed propagation distance and a constant height above the ground, it may be reasonable to assume that $C_n^2(z'\cos\alpha)$ is essentially constant.[24] Let us fix the radius to $r'=\omega(z)\sqrt{|l_0|/2}$; after normalization, we obtain the following simplified expression for the OAM spectrum:

$$P(l|l_0) = \frac{C_l}{\sum_{m=-\infty}^{\infty} C_m} = \frac{\mathrm{I}_{l-l_0}\left(\frac{2r'^2}{r_0^2}\right)}{\sum_{m=-\infty}^{\infty}\mathrm{I}_{m-l_0}\left(\frac{2r'^2}{r_0^2}\right)}. \quad (7)$$

3.2. Expression for the OAM spectrum under strong turbulence derived using the FRM

Unlike in the case of weak/medium turbulence, in a region with strong turbulence, the normalized complex amplitude of the beam can be expressed as[18]

$$\begin{aligned} &u_{l,\mathrm{strong}}(r,\phi,z)\\ &= u_{l,\mathrm{free}}(r,\phi,z)\exp[\psi_x(r,\phi,z)+\psi_y(r,\phi,z)], \end{aligned} \quad (8)$$

where $\psi_x(r,\phi,z)$ and $\psi_y(r,\phi,z)$ are the complex-phase perturbations caused by large- and small-scale turbulence eddies, respectively.

The most common method used to obtain the OAM probability density of any vortex beam under strong turbulence can be expressed as[18,19]

$$\begin{aligned} C_l = &\left(\frac{1}{2\pi}\right)^2\int_0^{2\pi}\int_0^{2\pi} u_{l,\mathrm{free}}(r,\phi,z)\,u_{l,\mathrm{free}}^*(r',\phi',z)\\ &\times\exp[-\mathrm{i}l(\phi-\phi')]\left\langle\exp[\psi_x(r,\phi,z)+\psi_y(r,\phi,z)\right.\\ &\left.+\psi_x^*(r',\phi',z)+\psi_y^*(r',\phi',z)]\right\rangle_{\mathrm{at}}\mathrm{d}\phi\,\mathrm{d}\phi', \end{aligned} \quad (9)$$

with

$$\begin{aligned} &\left\langle\exp[\psi_x(r,\phi,z)+\psi_y(r,\phi,z)\right.\\ &\left.+\psi_x^*(r',\phi',z)+\psi_y^*(r',\phi',z)]\right\rangle_{\mathrm{at}}\\ &= \exp\left[-\frac{1}{2}D(r,\phi,r',\phi',z)\right]\\ &= \exp\left[-\frac{1}{2}\left(D_x(r,\phi,r',\phi',z)+D_y(r,\phi,r',\phi',z)\right)\right]\\ &= \exp\left[-\frac{r^2+r'^2-2rr'\cos(\phi-\phi')}{\rho_0^2}\right], \end{aligned} \quad (10)$$

where ρ_0 is the spatial coherence radius in a channel with strong irradiance fluctuations and is given by[18]

$$\rho_0 = \left(0.491\sigma_{\mathrm{R}}^2\frac{k}{z}\left\{\left(\frac{35.046\eta_x z}{k\eta_x l_{\mathrm{i}}^2+35.046z}\right)^{1/6} +\left[1.766-\left(\frac{35.046\eta_y z}{k\eta_y l_{\mathrm{i}}^2+35.046z}\right)^{1/6}\right]\right\}\right)^{-1/2}, \quad (11)$$

with

$$\eta_x = \frac{8.56}{1+0.08\sigma_{\mathrm{R}}^2(10.89z/kl_{\mathrm{i}}^2)^{1/6}}$$

and

$$\eta_y = 9\left[1+0.69(0.4\sigma_{\mathrm{R}}^2)^{6/5}\right].$$

Here, l_{i} is the inner scale of the turbulence, and $\sigma_{\mathrm{R}}^2 = 1.23C_n^2(z)k^{7/6}z^{11/6}$ is the Rytov variance. Based on the integral expression[18]

$$\begin{aligned} &\int_0^{2\pi}\exp[-\mathrm{i}n\varphi_1+\eta\cos(\varphi_1-\varphi_2)]\,\mathrm{d}\varphi_1\\ &= 2\pi\exp(-\mathrm{i}n\varphi_2)\mathrm{I}_n(\eta), \end{aligned} \quad (12)$$

we can combine Eqs. (3), (8), (9), (10), and (11) to derive the expression for the OAM probability density of an LG beam under strong turbulence as follows:

$$\beta_l = \left(\frac{1}{2\pi}\right)^2\left[\frac{A}{\omega(z)}\right]^2\left[\frac{\sqrt{2}r}{\omega(z)}\right]^{2|l_0|}\exp\left[\frac{-2r^2}{\omega(z)^2}\right] \times\exp\left(-\frac{2r^2}{\rho_0^2}\right)\times 2\pi\mathrm{I}_{l-l_0}\left(\frac{2r^2}{\rho_0^2}\right). \quad (13)$$

We can also derive the expression for the OAM spectrum under strong turbulence as follows:

$$P(l|l_0)=\frac{\left\langle|\beta_l|^2\right\rangle}{\sum_{m=-\infty}^{\infty}\left\langle|\beta_m|^2\right\rangle}=\frac{\int_0^R\left[\frac{\sqrt{2}r}{\omega(z)}\right]^{2|l_0|}\exp\left[\frac{-2r^2}{\omega(z)^2}\right]\exp\left(-\frac{2r^2}{\rho_0^2}\right)\mathrm{I}_{l-l_0}\left(\frac{2r^2}{\rho_0^2}\right)r\mathrm{d}r}{\sum_{m=-\infty}^{\infty}\int_0^R\left[\frac{\sqrt{2}r}{\omega(z)}\right]^{2|l_0|}\exp\left[\frac{-2r^2}{\omega(z)^2}\right]\exp\left(-\frac{2r^2}{\rho_0^2}\right)\mathrm{I}_{m-l_0}\left(\frac{2r^2}{\rho_0^2}\right)r\mathrm{d}r}. \tag{14}$$

This is the EFM result for strong turbulence. Using the FRM, we fix the radius to r' and obtain the following simplified expression for the OAM spectrum under strong turbulence:

$$P(l|l_0)=\frac{\mathrm{I}_{l-l_0}\left(\frac{2r'^2}{\rho_0^2}\right)}{\sum_{m=-\infty}^{\infty}\mathrm{I}_{m-l_0}\left(\frac{2r'^2}{\rho_0^2}\right)}. \tag{15}$$

4. Analysis of the validity of the FRM in channels with atmospheric turbulence

In this section, we demonstrate the validity of the FRM. We consider several OAM spectra, as depicted in Fig. 2, which show the proportion of the power that remains in the transmitted OAM state or leaks into other states via crosstalk. We set the parameters as follows: $\omega_0=0.01$ m, $\lambda=1550$ nm, $z=500$ m, $v=21$ m/s and the zenith angle is set to $\alpha=\pi/2$, which indicates that the beam is transmitted horizontally, and consequently, equation (6) becomes a function of only z. Considering typical manufacturing limitations and the size of a typical receiver, we set the receiver aperture radius to $R=10$ cm.[25] Figures 2(a) and 2(b) present the OAM spectra for different transmitted OAM numbers under weak/medium and strong turbulence, respectively. Because most of the power is concentrated around state l_0, only finite terms are considered. We use 21 and 61 states around l_0 to calculate the results of Eqs. (7) and (15), respectively. For comparison, we also present the results obtained using the EFM. As shown in Fig. 2, the results of the two methods are consistent, particularly for larger OAM numbers.

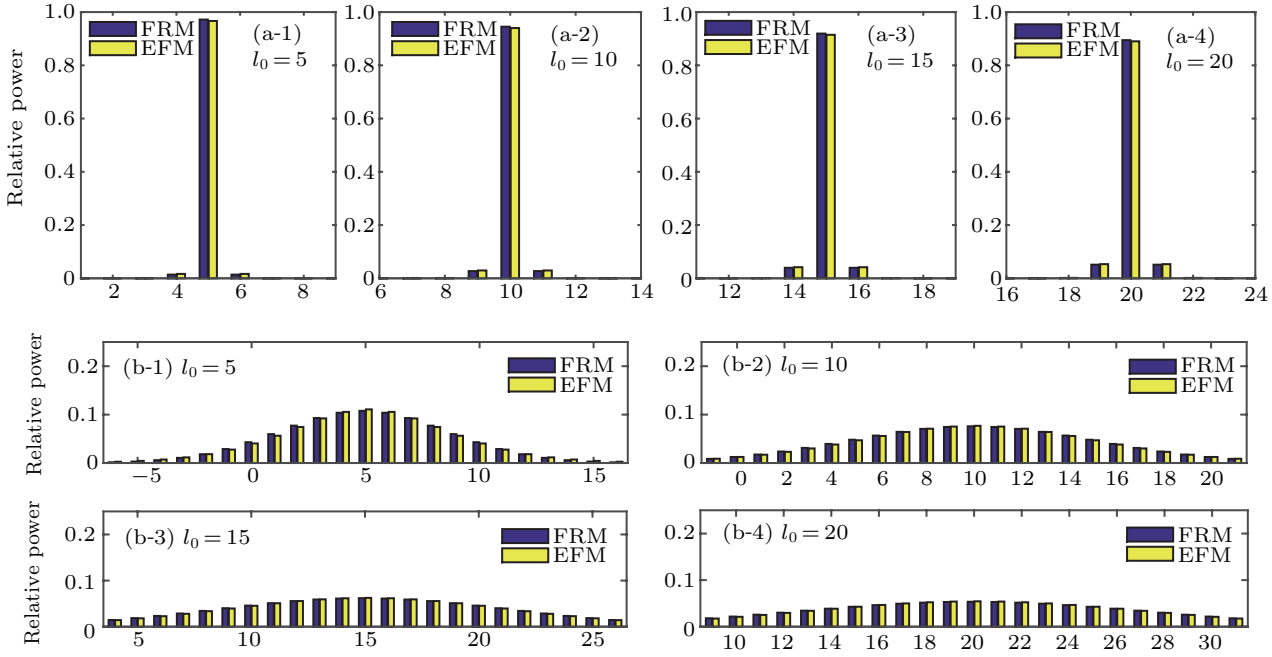


Fig. 2. (color online) OAM spectra for $l_0=5$, 10, 15, 20 under different levels of turbulence: (a) weak/medium turbulence, $C_n^2(0)=10^{-15}$ m$^{-2/3}$; (b) strong turbulence, $C_n^2(0)=10^{-13}$ m$^{-2/3}$.

To quantitatively compare the EFM and FRM results, a dimensionless parameter called the overall error is defined as follows:

$$e=\sum_{l=-\infty}^{\infty}|P_{\mathrm{EFM}}(l|l_0)-P_{\mathrm{FRM}}(l|l_0)|. \tag{16}$$

We do not need to normalize the parameter e because the sum of the entire OAM spectrum is equal to 1. The value of e lies between 0 and 1, and a smaller e corresponds to more accurate FRM results. Figure 3 shows the overall error versus turbulence for $l_0=5$, 10, 15, and 20. We use 21 and 61 states around l_0 to calculate the results of Eq. (16) for weak/medium and strong turbulence, respectively.

None of the e values in Fig. 3 exceeds 0.05. For example, the overall error corresponding to Fig. 2(b-1) is 0.0425, and the results also appear visually identical; furthermore, this figure shows that even the worst situation can be accepted.

Thus, the results of the two methods are nearly identical for both weak/medium and strong turbulence. In Fig. 3(a), under weak/medium turbulence, the overall error increases gradually with increasing $C_n^2(0)$, and at larger OAM numbers, the overall error is smaller. By contrast, the errors in Fig. 3(b) are nearly ten times of those in Fig. 3(a), and the overall errors remain nearly steady. Thus, the overall error initially increases as $C_n^2(0)$ increases and remains steady once $C_n^2(0)$ reaches the strong turbulence range. Therefore, we can conclude from Fig. 3 that the accuracy of the FRM is acceptable under any level of turbulence, particularly in situations with weaker turbulence, when the OAM number is sufficiently large.

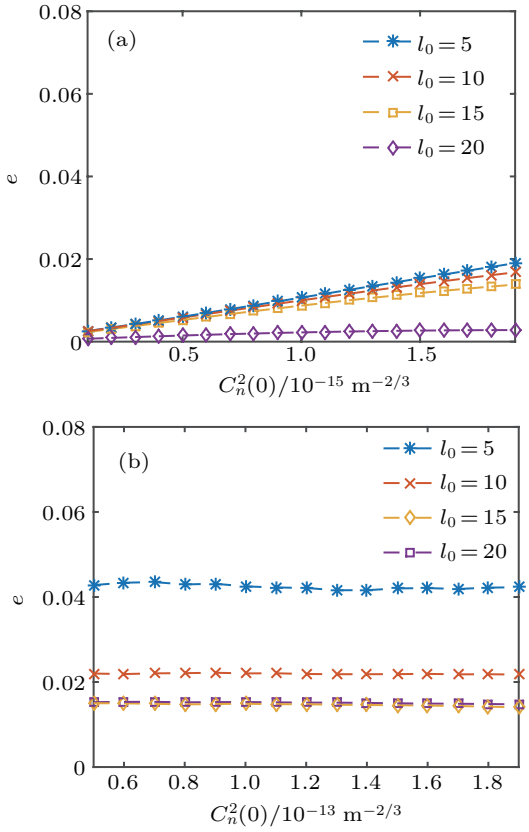


Fig. 3. (color online) Overall error e for $l_0 = 5$, 10, 15, and 20: (a) weak/medium turbulence, (b) strong turbulence.

Figure 4 shows the overall error versus the OAM number l_0 for weak/medium and strong turbulence. Figure 4(a) shows that for a given turbulence, e gradually decreases as l_0 increases, particularly under strong turbulence. In the range of small OAM numbers, the overall error remains nearly constant, whereas e drastically decreases as l_0 increases in Fig. 4(b). For small OAM numbers ($l_0 \leq 5$) and strong turbulence, as shown in Fig. 4(b), the overall errors exceed 0.1, and the accuracy is low. This is because when the OAM number is small, the ring over which the beam intensity is distributed is thick, and strong turbulence causes the intensity distribution to deviate from an annulus. Thus, we can conclude from Fig. 4 that when l_0 is larger, the overall error is smaller, and the FRM method is not suitable (when e exceeds 0.1) for small OAM numbers ($l_0 \leq 5$) and strong turbulence.

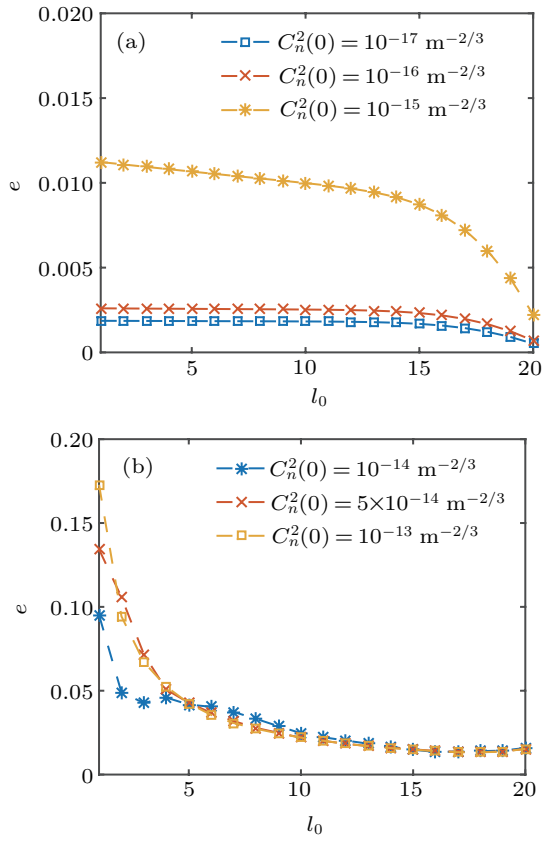


Fig. 4. (color online) Overall error e of the OAM spectrum calculations in different situations: (a) weak/medium turbulence, (b) strong turbulence.

In conclusion, the proposed simplified expressions for the OAM spectrum are highly accurate, particularly for weak turbulence and large OAM numbers.

5. Discussion

Based on the simplified expressions for the OAM spectrum, we can analytically investigate the rules governing the variation of the OAM spectrum with the OAM number l_0 and the turbulence strength.

Interestingly, the results of Eqs. (7) and (15) are similar, except for the expression of the coherence radius. Because $\mathrm{I}_{-\alpha}(x) = \mathrm{I}_{\alpha}(x)$,[1] we can write a single simplified expression for the OAM spectrum under either weak/medium or strong turbulence as follows:

$$P[(l_0+m)|l_0] = \frac{\mathrm{I}_m(x)/\mathrm{I}_0(x)}{1+2\times\sum_{n=1}^{\infty}[\mathrm{I}_n(x)/\mathrm{I}_0(x)]}, \tag{17}$$

where m is the OAM number adjacent to the transmitted l_0 and

$$x = \begin{cases} \dfrac{2r'^2}{r_0^2} = \dfrac{\omega(z)^2|l_0|}{r_0^2}, & \text{for weak/medium turbulence,} \\ \dfrac{2r'^2}{\rho_0^2} = \dfrac{\omega(z)^2|l_0|}{\rho_0^2}, & \text{for strong turbulence.} \end{cases} \tag{18}$$

Equation (18) shows that x is directly proportional to $|l_0|$ and inversely proportional to r_0^2 or ρ_0^2. The remaining relative power in the transmitted OAM state $|l_0|$ can be expressed as

$$P(l_0|l_0) = \frac{1}{1+2\times\sum_{n=1}^{\infty}\left[\mathrm{I}_n(x)/\mathrm{I}_0(x)\right]}. \tag{19}$$

Equations (17) and (19) show that when x is fixed, the OAM spectrum will remain the same. Thus, an increase in l_0 at a fixed level of turbulence can induce an effect identical to that caused by an increase in $C_n^2(0)$ at a fixed l_0. Consequently, we can obtain the same OAM spectrum by either increasing l_0 or decreasing $C_n^2(0)$.

According to Eq. (18), if the turbulence and transmission distance are known, which implies that ρ_0 or r_0 is fixed because x is directly proportional to $|l_0|$, an increase in the transmitted OAM number l_0 causes x to increase. From Eqs. (17) and (19), we can see that the OAM spectrum depends on the ratio $\mathrm{I}_m(x)/\mathrm{I}_0(x)$. To show the relationship between l_0 and the OAM spectrum at a fixed level of turbulence, we numerically calculate $\mathrm{I}_m(x)/\mathrm{I}_0(x)$ for $m = 0$, 1, 2, 3, 4, and 5, with $C_n^2(0) = 5\times10^{-15}$ m$^{-2/3}$ and $z = 1000$ m. The calculation results are shown in Fig. 5. Figure 5 shows that $\mathrm{I}_m(x)/\mathrm{I}_0(x)$ monotonically increases with l_0 and when m increases, $\mathrm{I}_m(x)/\mathrm{I}_0(x)$ decreases.

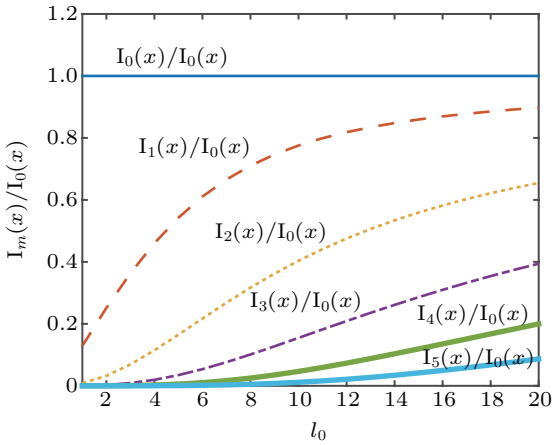


Fig. 5. (color online) The $\mathrm{I}_m(x)/\mathrm{I}_0(x)$ for $m = 0$, 1, 2, 3, 4, and 5.

For Eq. (17) with $m \neq 0$, some power leaks into other OAM states. When l_0 and the turbulence are fixed, we can compare the power leaking to adjacent OAM numbers simply by comparing $\mathrm{I}_m(x)/\mathrm{I}_0(x)$ because the denominator of Eq. (17) is constant. In Fig. 5, when m increases, $\mathrm{I}_m(x)/\mathrm{I}_0(x)$ decreases. Thus, the relative power in the OAM spectrum is related to the distance of the OAM number from l_0; as the OAM number moves away from l_0, the power that leaks to it decreases. Thus, in Fig. 2, the turbulence-disturbed OAM spectrum assumes a bell-like shape, being tall in the center and declining on the sides.

According to Eq. (19), the remaining relative power in the transmitted OAM state $P(l_0|l_0)$ decreases as l_0 increases, as shown in Figs. 2(a) and 2(b). We can also consider crosstalk with other OAM states based on Eq. (19), where $\mathrm{I}_m(x)/\mathrm{I}_0(x)$ is included in $\sum_{n=1}^{\infty}\left[\mathrm{I}_n(x)/\mathrm{I}_0(x)\right]$. Therefore, an increase in l_0 will cause $P(l_0+m|l_0)$ to decrease. Thus, the curves in Fig. 2 become flatter as l_0 increases.

To show the relationship between $C_n^2(0)$ and the OAM spectrum, we also plot the curves of $\mathrm{I}_m(x)/\mathrm{I}_0(x)$ for different $C_n^2(0)$ with a transmitted OAM number of $l_0 = 15$ and a transmission distance of $z = 1000$ m in Fig. 6.

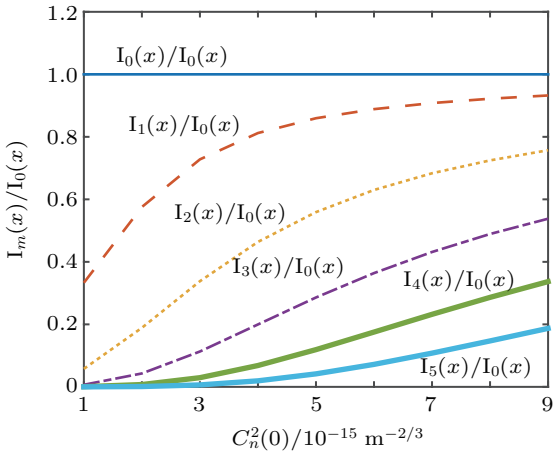


Fig. 6. (color online) The $\mathrm{I}_m(x)/\mathrm{I}_0(x)$ for $m = 0$, 1, 2, 3, 4, and 5.

In Fig. 6, $\mathrm{I}_m(x)/\mathrm{I}_0(x)$ monotonically increases with increasing $C_n^2(0)$ and decreases as m increases, which is identical to the behavior observed with increasing l_0 and m in Fig. 5. As seen from Eqs. (17) and (19), for a fixed l_0 and a fixed transmission distance z, r_0 and ρ_0 vary inversely with $C_n^2(0)$. Thus, an increase in $C_n^2(0)$ causes $\mathrm{I}_m(x)/\mathrm{I}_0(x)$ to decrease, implying that an increase in turbulence will cause the entire OAM spectrum to become lower in peak power and exhibit increased broadening.

6. Conclusion and perspectives

We propose the FRM for deriving simplified expressions for the OAM spectrum. We fix the radius of the OAM beam to the extreme point of the intensity distribution to make the expressions more concise and reduce the amount of calculation. Then, we define an overall error e to measure the accuracy of the FRM results. Based on this error calculation, we find that the FRM has high accuracy, particularly for large transmitted OAM numbers. However, the overall error is relatively large when the transmitted OAM number is small ($l_0 \leq 5$) and the turbulence is strong. Finally, we demonstrate that the broadening of the OAM spectrum caused by atmospheric turbulence can be studied analytically using the proposed simplified ex-

pressions. Moreover, a concise expression without infinite integration will be important for future derivations of channel matrices and simulations of multiplexed FSO-OAM systems.

References

[1] Ke X Z, Chen J and Yang Y M 2014 *Acta Phys. Sin.* **63** 150301 (in Chinese)

[2] Alan E W, Xie G D, Li L, Ren Y X, Yan Y, Nisar A, Zhao Z, Wang Z, Liu C, Asher J W, Nima A, Solyman A, Moshe T and Andreas F M 2016 *Journal of Optics* **18** 074014

[3] Graham G, Johannes C, Miles J P, Mikhail V, Valeriy P, Stephen M B and Sonja F A 2004 *Opt. Express* **12** 5448

[4] Wang J, Yang J Y, Irfan M F, Nisar A, Yan Y, Huang H, Ren Y X, Yue Y, Samuel D, Moshe T and Willner A E 2012 *Nat. Photon.* **6** 488

[5] Mario K, Robert F, Matthias F, Johannes H, Mehul M, Thomas S, Rupert U and Anton Z 2014 *New J. Phys.* **16** 113028

[6] Zhao Y F, Liu J, Du J, Li S H, Luo Y, Wang A D, Zhu L, and Wang J 2016 *Optical Fiber Communication Conference*, March 20–22, 2016, California, United States, pp. Th1H.3

[7] Mario K, Johannes H, Matthias F, Robert F, Rupert U, Mehul M and Anton Z 2016 *Proc. Natl. Acad. Sci. USA* **113** 13648.

[8] Paterson C 2005 *Phys. Rev. Lett.* **94** 153901

[9] Zhang Y X, Zhao G Y, Xu J C and Cuang J 2009 *Wri International Conference on Communications and Mobile Computing*, January 6–8, 2009, Kunming, China, pp. 477–481

[10] Zhang Y X, Wang Y G, Xu J C, Wang J Y and Ji J J 2011 *Opt. Commun.* **284** 132

[11] Miles J P, Filippo M M, Martin L, Anton Z and Robert W B 2015 *New J. Phys.* **17** 023011

[12] Anguita J A, Neifeld M A and Vasic B V 2008 *Appl. Opt.* **47** 2414

[13] Yin X L, Sang H Q, Cui X Z, Chang H, Li L and Wu G H 2017 *Opt. Commun.* **393** 34

[14] Dios F, Rubio J A, Rodríguez A and Comerón A 2004 *Appl. Opt.* **43** 3866

[15] Noll R J 1976 *J. Opt. Soc. Am.* **66** 207

[16] Miller W B, Andrews L C and Ricklin J C 1994 *Josa A* **11** 2719

[17] Zhang Y X, Wang Y G, Xu J C, Wang J Y and Ji J J 2011 *Opt. Commun.* **284** 1132

[18] Gao J, Zhang Y, Dan W and Hu Z 2015 *Opt. Express* **23** 17024

[19] Zhu Y, Zhang Y and Hu Z 2016 *Opt. Express* **24** 10847

[20] Jiang Y S, Wang S H, Zhang J H, Ou J and Tang H 2013 *Opt. Commun.* **16** 38

[21] Zhang Y, Cheng M, Zhu Y, Gao J, Dan W and Hu Z 2014 *Opt. Express* **22** 22101

[22] Cheng M, Guo L, Li J and Huang Q 2016 *J. Opt. Soc. Am.* **33** 1442

[23] Zou L, Wang L, Zhao S M and Chen H W 2016 *Chin. Phys. B* **25** 114215

[24] Andrews L C and Phillips R L 2005 *Laser Beam Propagation through Random Media* (2nd Edn.) September 16, 2005, Washington, United States, p. 481

[25] Toyoshima M 2005 *Journal of Optical Networking* **350** 300